tallographic axes. It is possible that it is this difficulty which explains why no such anomalies were observed so far.

In conclusion, we take the opportunity to thank I. M. Lifshitz and L. P. Pitaevskiĭ for stimulating discussions.

[1)]The lines of parabolic points are the border lines between Fermi-surface sections having Gaussian curvatures of opposite sign. At the parabolic point, one of the principal curvatures of the surface reverses sign. A parabolic point is a point where the surface flattens.

[2)]The propagation and absorption of sound in metals whose Fermi surfaces contain degenerate parabolic points were considered in Refs. 5 and 6 with chalcogenides as examples.

[3)]The critical-direction cone can be constructed by moving along a line of parabolic points.

[4)]In the case of a spherical Fermi surface, assuming that Λ does not depend on the angles, we easily obtain from (4)

$$\Gamma_e = \frac{2k|\Lambda|^2\pi^2 p_F^2}{\rho(2\pi\hbar)^3 v_F^2} = \frac{2k|\Lambda|^2\pi^2(m^*)^2}{\rho(2\pi\hbar)^3}, \quad m^* = \frac{p_F}{v_F}.$$

If we assume $\Lambda \approx p_F^2/m^*$, $p_F \approx \hbar/a$, $\rho \approx M/a^3$, $m^* \approx m_0$ (m_0 is the mass of the free electron, M is the mass of the ion metal, and a is the interatomic distance), and $s^2 = (m_0/M)v_F^2$, then $\Gamma_e/\omega \approx (m_0/M)^{1/2}$. This is only an order-of-magnitude equality, and it determines the scale of the electronic part of the sound absorption coefficient.

[5)]In this system the coordinates of the parabolic point are $p_x = p_z = 0$ and $\varepsilon = 0$.

[6)]This is most unlikely, since the parabolic points do not have high symmetry (see above, as well as Ref. 6).

[7)]It is seen from the very same figure that at certain directions of $\mathbf{n}$ ($\mathbf{n}_1$ in the figure) the number of periods can decrease because of the symmetry of the Fermi surface, which causes some extremal diameters to coincide.

[8)]We measure p_z from that value at which $\Delta^{ij}p_y(p_z)$ has an extremum.

[1]A. I. Akhiezer, M. I. Kaganov, and G. Ya. Lyubarskiĭ, Zh. Eksp. Teor. Fiz. 32, 837 (1957) [Sov. Phys. JETP 5, 685 (1957)].
[2]M. Ya. Azbel' and M. I. Kaganov, Dokl. Akad. Nauk SSSR 95, 41 (1954).
[3]I. M. Lifshitz, M. Ya. Azbel', and M. I. Kaganov, Élektronnaya teoriya metallov (Electron Theory of Metals), Nauka, 1971.
[4]G. T. Avanesyan, M. I. Kaganov, and T. Yu. Lisovskaya, Pis'ma Zh. Eksp. Teor. Fiz. 25, 381 (1977) [JETP Lett. 25, 355 (1977)].
[5]V. M. Kontorovich and N. A. Sapogova, Pis'ma Zh. Eksp. Teor. Fiz. 18, 381 (1973) [JETP Lett. 18, 223 (1973)].
[6]N. A. Stepanova, Fiz. Nizk. Temp. 3, 1415 (1977) [Sov. J. Low Temp. Phys. 3, 680 (1977)].
[7]A. B. Pippard, Philos. Mag. 46, 1104 (1955).
[8]V. L. Gurevich, Zh. Eksp. Teor. Fiz. 37, 71 (1959) [Sov. Phys. JETP 10, 51 (1960)].

Translated by J. G. Adashko

Symmetry of "current" states and spontaneous oscillations in bismuth

G. I. Babkin, V. T. Dolgopolov, and P. N. Chuprov

Institute of Solid-State Physics, Academy of Sciences of the USSR, Moscow

(Submitted 30 May 1978)
Zh. Eksp. Teor. Fiz. **75**, 1801–1811 (November 1978)

Irradiation of a metal plate with radio waves may produce a macroscopic magnetic moment in zero magnetic field, i.e., it may induce a transition to a "current" state. A calculation is given of the width and position of hysteresis loops which appear because of the induced magnetic moment. A study is made of the stability of the current states and it is shown that—under certain conditions—periodic oscillations of the magnetic moment may be expected. A report is given of measurements carried out on bismuth in which such spontaneous oscillations were observed experimentally.

PACS numbers: 78.70.Gq, 75.60.Ej, 75.70.Kw

Irradiation of a metal plate with radio waves may produce a macroscopic magnetic moment because of rectification of the rf current.[1,2] The inequivalence of two consecutive half-periods of the rf current is due to the presence of a static magnetic field. When the magnetic field created by the rectified current itself is sufficient to maintain the rectification process, a sample retains a magnetic moment even in zero magnetic field. A metal can then assume at least two "current" states which differ in respect to the direction of the rectified current and, consequently, in respect to the sign of the magnetic moment of the sample. Application of an external magnetic field anti-parallel to the magnetic moment causes a sudden transition from one current state to the other. The dependence of the magnetic moment on an external magnetic field in the presence of an additional large-amplitude alternating field exhibits a hysteresis loop. This behavior has been observed experimentally and investigated in bismuth and tin.[1,2]

The rectification mechanism, which produces such current states, was proposed by us earlier.[3] In one of the half-periods of the alternating field when the external magnetic field is antiparallel to the alternating field, an open trajectory shown in Fig. 1b appears near the surface. Electrons moving along this trajectory enter more frequently the skin layer than those moving

 0038-5646/78/110907-06$02.40

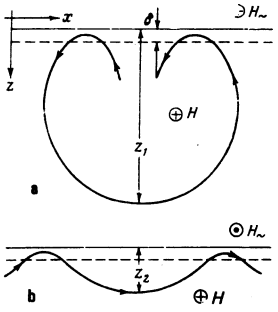

FIG. 1. Trajectories of the effective electrons during different half-periods of the rf field.

along a slightly distorted usual Larmor orbit (Fig. 1a). An increase in the number of times that an electron returns to the skin layer increases the effective conductivity during this period and gives rise to a rectified current.

In metals with a complex Fermi surface a change in the contribution made to the rectification effect by one of the electron groups affects the efficiency of rectification by other electron groups. Therefore, the dependence of the widths and positions of the hysteresis loops on the direction of the external magnetic field may become quite complex. We shall calculate the widths and positions of the hysteresis loops in bismuth. We shall derive the angular dependence of the width of the central hysteresis loop, which agrees qualitatively with the experimental results, and explain the origin of the observed[1] side hysteresis loops.

We shall also consider the stability of various current states. In a spatially inhomogeneous magnetic field the rectified current depends on the magnetic field at two characteristic points denoted by z_1 and z_2 in Fig. 1. A change in the magnetic field at any point on the electron orbit alters practically instantaneously the rectification efficiency in a time of the order of the electron relaxation time $\tau \ll \omega^{-1}$, where ω is the frequency of the alternating (rf) field. The change in the rectified current affects the field at the points $z_{1,2}$ after times of the order of $\tau_{1,2} \sim \sigma z_{1,2}^3/c^2 r$ (σ is the conductivity and r is the Larmor orbit radius), which exceed considerably τ and differ very greatly: $\tau_1 \gg \tau_2$. Under these conditions we may expect spontaneous oscillations of the rectified current and, consequently, similar oscillations of the magnetic moment of the sample at frequencies $\tilde{\omega}$, such that the phase shift $\tilde{\omega}(\tau_1 - \tau_2) \gg 1$ is large and any phase relationship can be satisfied.

We shall show that when the amplitude of the alternating field is sufficiently large, such spontaneous oscillations can indeed be observed. We shall report experiments carried out on bismuth samples which confirm the appearance of such oscillations.

CALCULATION OF THE WIDTH AND POSITION OF HYSTERESIS LOOPS FOR THE FERMI SURFACE MODEL OF BISMUTH

The expression for the magnetic field $\mathcal{H}$ created by a rectified current in a metal with a cylindrical Fermi surface, obtained in Ref. 3, is valid for $H_\sim \gg H$, where $H_\sim$ is the amplitude of the projection of the alternating

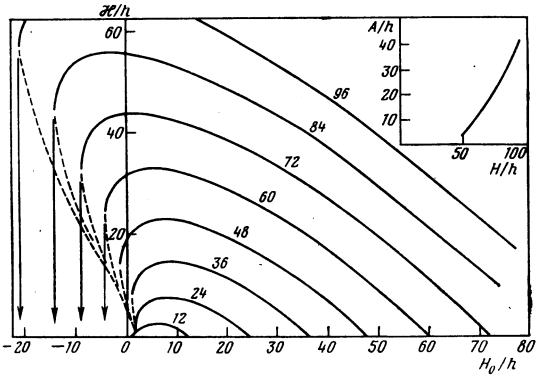

FIG. 2. Dependence of the field $\mathcal{H}$ created by the rectified current on the external magnetic field H_0. The numbers alongside the curves give the amplitude of the rf field in relative units $H_\sim/h$. The inset shows the width A of a hysteresis loop as a function of the rf field amplitude $H_\sim$

field and H is the projection of the total magnetic field on the cylinder axis.

We shall need the dependence $\mathcal{H}(H)$ in the range $H \lesssim H_\sim$. We shall bear in mind that the trajectory responsible for the appearance of the current states exists as long as

$$\int_0^\infty H_\sim(z)\,dz = H_\sim(0)\,\delta \sin\varphi > H\delta,$$

i.e., it exists when the phase φ is within the limits

$$\varphi_1 = \arcsin(H/H_\sim) \leqslant \varphi \leqslant \pi - \arcsin(H/H_\sim) = \varphi_2.$$

On the strength of this inequality we have, instead of Eqs. (3) and (4) in Ref. 3,

$$\mathcal{H} = \frac{H_\sim}{2\pi}\int_{\varphi_1}^{\varphi_2} \sin\left(\varphi - \frac{\pi}{6}\right)\left[\exp\frac{T(\varphi)}{\tau} - 1\right]^{-1} d\varphi = f(H_\sim, H),$$

$$T(\varphi) = \tau h^{1/h}[(H_\sim \sin\varphi)^{1/h} H^{-1} + (H_\sim \sin\varphi)^{-1/h}], \qquad (1)$$

$$h = mc\delta/e\tau l,\ H = H_0 \cos\alpha + \mathcal{H},$$

where l and m are, respectively, the mean free path and the electron mass; δ is the skin depth, H_0 is the external magnetic field. The differences which appear as a result of changes in the integration limits are important only for $H \gtrsim 0.3H_\sim$. Graphs of the dependence $\mathcal{H}(H_0)$ are given in Fig. 2 for several values of $H_\sim$. The dashed parts of the curves are those in which the state of a sample is unstable.

In our calculations we shall assume that the electron part of the Fermi surface of bismuth consists of three cylindrical surfaces. Ignoring the 6° slope, we shall assume that the cylinder axis lie in the same plane and meet at 120°. In accordance with the experimental conditions,[1] we shall assume that the rf current is directed along one of the cylinder axes. Then, electrons in this cylinder make no contribution at all to the current (because the electron velocity is perpendicular to the direction of the current) and the contributions of the other two cylinders are equal and depend weakly on H as long as $eH\tau/mc \lesssim 1$. We shall use $\mathcal{H}_1$ and $\mathcal{H}_2$ to denote the static fields which appear because of changes in the electron trajectories in various cylinders. These fields, directed along the cylinder axes, can be found from the

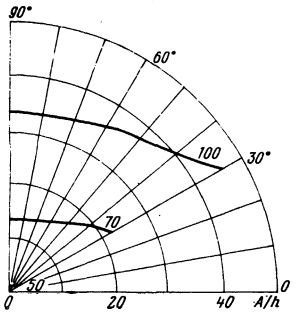

FIG. 3. Dependences of the width A of a hysteresis loop on the direction of external magnetic field (angle $\psi = 0$ for $\mathbf{H}_0 \| \mathbf{j}$). The number alongside each curve gives the rf magnetic field amplitude in relative units $H_\sim/h$.

system

$$\mathcal{H}_1 = \beta f(H_\sim \cdot 3^{1/2}/2,\ H_0 \cos(\pi/3-\psi) + \mathcal{H}_1 - \mathcal{H}_2/2),$$
$$\mathcal{H}_2 = \beta f(H_\sim \cdot 3^{1/2}/2,\ H_0 \cos(\pi/3+\psi) + \mathcal{H}_2 - \mathcal{H}_1/2). \quad (2)$$

Here, f is the function which specifies, in accordance with Eq. (1), the relationship between $\mathcal{H}$ and H in the case of one cylinder; the angle Ψ is measured from the direction of the rf current. The coefficient β allows for the contribution of holes to the rf conductivity. (If this contribution is ignored, then $\beta = 2/3$.)

There is a sudden change in the rectified current at those values of H_0 and Ψ when at least one of the derivatives $\partial\mathcal{H}_{1,2}/\partial H_0 = \mathcal{H}'_{1,2}$ becomes infinite. Differentiating Eq. (2) and equating to zero the determinant of the resultant system, we obtain

$$(f_1'-1)(f_2'-1) - f_1' f_2'/4 = 0; \quad (3)$$
$$f_1' = \beta f'(H_0 \cos(\pi/3-\psi) + \mathcal{H}_1 - \mathcal{H}_2/2),$$
$$f_2' = \beta f'(H_0 \cos(\pi/3+\psi) + \mathcal{H}_2 - \mathcal{H}_1/2).$$

The system (1)–(3) determines the dependence, on the angle Ψ, of the external field in which the magnetic moment of the sample changes abruptly. For each value of Ψ there may be several abrupt changes in a magnetic moment and, therefore, in determining the width of a hysteresis loop we have to select a jump corresponding to the highest magnetic field. Figure 3 shows the dependence of the hysteresis loop width on the magnetic field direction in the range $\pi/6 \leq \Psi \leq \pi/2$, obtained by numerical solution of Eqs. (1)–(3) for $\beta = 2/3$. The curves in Fig. 3 are only in qualitative agreement with the experimental results. A better agreement cannot be expected because of the large number of the simplifying assumptions made in the calculations.

The dependences of the parameters of a side hysteresis loop on the direction of the external magnetic field are less sensitive to the precision of the calculations. The origin of this loop can easily be deduced from the fact that the projection of the total field $\mathbf{H} = \mathbf{H}_0 + \vec{\mathcal{H}}_1 + \vec{\mathcal{H}}_2$ onto the axis of one of the cylinders can alter the sign in a relatively high external field H_1. Since the number of times that an electron returns to the skin layer depends only on the projection of the total magnetic moment on the cylinder axis, it follows that for electrons in this cylinder the field H_1. Since the number of times that an electron returns to the skin layer depends only on the projection of the total magnetic moment on the cylinder axis, it follows that for electrons in this cylinder the field H_1 is indistinguishable from zero.

The value of the field H_1 is found by substituting

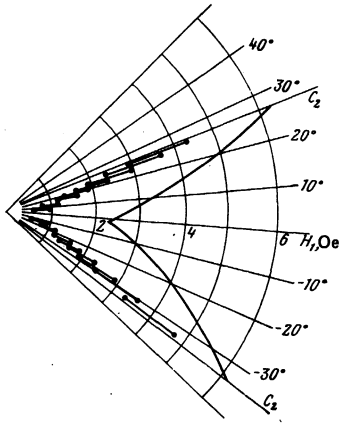

FIG. 4. Comparison of the calculated (continuous curve) and experimental dependences $H_1(\psi)$; $H_\sim = 7.2$ Oe, $h = 0.06$ Oe, which corresponds to $\delta = 2\times10^{-3}$ cm, $\tau = 5\times10^{-10}$ sec, $\beta = 2/3$; $\psi = 0$ for $\mathbf{H}_0 \| \mathbf{j}$.

$\mathcal{H}_2 = 0$ in Eq. (2):

$$\mathcal{H}_1 = 2H_1 \cos(\pi/3+\psi),\ \mathcal{H}_1 = \beta f(H_\sim \cdot 3^{1/2}/2,\ H_1 \cos(\pi/3-\psi) + \mathcal{H}_1). \quad (4)$$

Figure 4 shows how the experimental results compare with the dependence $H_1(\Psi)$ calculated from Eqs. (1) and (4) ignoring the contribution of holes to the rf conductivity. It is clear from this figure that, on the average, the calculated value is twice the experimental result.

The experimental and theoretical curves can be made to agree if β is treated as the adjustable parameter. However, in our view, a different approach is more interesting: we can use Eq. (4) to plot the function $f(H_0)$ using the experimental dependence $H_1(\psi)$. The experimental points in Fig. 4 are used in the dependence $\mathcal{H}(H_0) = 2\beta f(H_\sim \cdot 3^{1/2}/2, H_0/2)$ as shown in Fig. 5. This figure includes also a continuous curve obtained experimentally by a different and independent method. According to our model, the dependence $\mathcal{H}(H_0)$ should be proportional to the magnetization of the sample in the $\mathbf{H}_0 \perp j$, $C_1 \| j$ case, and the magnetization can be found experimentally. This was done by recording the curves $(\partial\mathcal{H}/\partial H_\sim)H_\sim$, corresponding to various values of $H_\sim$. [The signal proportional to $(\partial\mathcal{H}/\partial H_\sim)H_\sim$ appeared in an inductance coil surrounding a sample when the alternating field was subjected to weak low-frequency modulation.] A set of the $(\partial\mathcal{H}/\partial H_\sim)H_\sim$ curves, some of which are shown in Fig. 6, could be subjected to numerical integration and the dependence $\mathcal{H}(H_0)$ could be found in this way; however, this would be subject to an unknown numerical factor. It is clear from Fig. 5 that

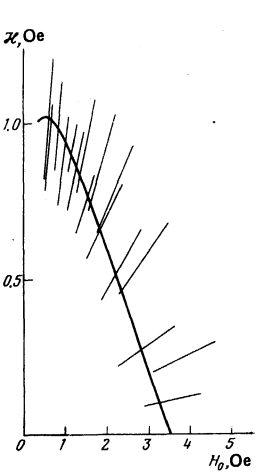

FIG. 5. Dependence $\mathcal{H}(H_0)$ plotted using the results of two experiments; $c_3 \| \mathbf{n}$, $d = 0.4$mm, $\mathbf{j} \| c_1$, $H_\sim = 7.2$ Oe.

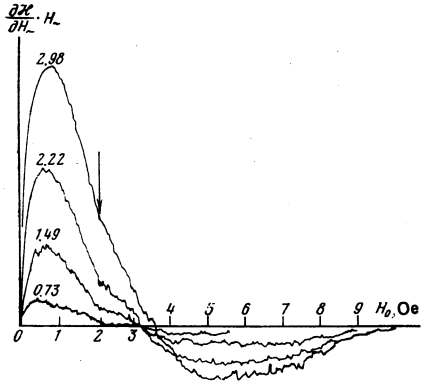

FIG. 6. Dependence of $(\partial\mathcal{H}/\partial H_\sim)H_\sim$ on an external magnetic field applied to a sample 0.4 mm thick; $\mathbf{H}_0 \perp \mathbf{j} \| c_1$, $T = 1.3°K$. The number alongside the curve is the rf field amplitude in oersted.

the curve obtained in this way could be fitted, within the limits of the experimental error, to the points derived from the angular dependence of the position of a hysteresis loop. This justified the adopted approximation and, moreover, gave a calibration coefficient. The precision of the calibration was about 10%. The calibration coefficient enabled us to plot in absolute units the dependence $\mathcal{H}(H_0)$ for arbitrary values of $H_\sim$ (Fig. 7).

STABILITY OF THE CURRENT STATES AND SPONTANEOUS OSCILLATIONS

We shall assume that an inhomogeneous correction $\Delta\mathcal{H}$ to the field $\mathcal{H}$ appears in a sample because of the rectification-induced magnetic moment. We shall find the time dependence of this correction. (For simplicity, we shall again use the cylindrical model of the Fermi surface.) We shall first consider the appearance of an instability at the lowest frequencies, when $\Delta\mathcal{H}$ changes only slightly over distances of the order of the characteristic size $z_{1,2}$ of the electron trajectories (Fig. 1). Then,

$$f(\mathcal{H}+\Delta\mathcal{H}+H_0) = f(\mathcal{H}+H_0) + f'\Delta\mathcal{H} - bz_2 d(\Delta\mathcal{H})/dz, \qquad (5)$$

where $b > 0$ and the returns of electrons to the skin layer can be neglected for the circular orbit corresponding to Fig. 1a ($l \ll z_1$).

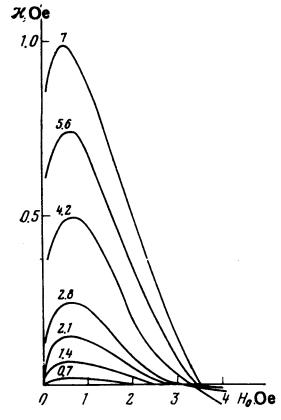

FIG. 7. Rectified-current field plotted as a function of an external magnetic field for different rf field amplitudes. The conditions are the same as in Fig. 6.

We shall consider a plate of thickness $2d$. If the time dependence is $\exp(i\tilde{\omega}t)$ and $\Delta\mathcal{H}$ satisfies the conditions for the normal skin effect, we obtain

$$\Delta\mathcal{H} = \Delta\mathcal{H}(0)\,\mathrm{ch}kz/\mathrm{ch}kd, \qquad (6)$$

where $c^2k^2/4\pi\sigma = i\tilde{\omega}$. Substituting Eqs. (6) and (5) into the equation $\mathcal{H} = f(H_0 + \mathcal{H})$, we find that at the point $z = d$:

$$(f'-1)bd/z_1 = kd\,\mathrm{th}kd. \qquad (7)$$

if $f' > 1$, this equation has a root for real values of k. The solution with this root rises exponentially with time which corresponds to the appearance of an instability. Moreover, there is an infinite set of solutions for purely imaginary values of k, which exists for $f' > 1$ and $f' < 1$. Such solutions are damped out with time, in complete agreement with the solutions for the ordinary Foucault currents.

Thus, if $l \ll z_1$, only those states are stable which are characterized by $f' < 1$. Therefore, it is not surprising that the states with $f' > 1$ are never observed experimentally. In the opposite limiting case of $l \gg z_1$ we have to allow for returns of electrons following the usual circular orbit. This allowance has practically no effect on f but it alters greatly the stability conditions. In the presence of long-wavelength perturbations the stable states are those with any value of f' with the exception of a narrow range defined by $1 - (z_2/z_1)^{1/2} \leq f' \leq 1$. However, we shall show later that when $f' > 1$ and $l \gg z_1$, the state of a sample is unstable in respect of excitation of spontaneous oscillations.

We shall now consider perturbations corresponding to higher frequencies $\tilde{\omega}$. As pointed out earlier, our system receives energy from an external source (rf field) and it may exhibit spontaneous oscillations. Systems of this kind are considered by Gurevich and Ioffe[4] for the case of a weakly attenuated energy flux. We shall discuss the opposite case when an electromagnetic wave is damped out over distances of $\delta \ll d$. We shall assume the skin effect to be anomalous at the frequency $\tilde{\omega}$. Since all possible solutions are damped out over distances of the order of $k^{-1} \ll d$, we shall confine our attention to the case when a sample occupies the half-space $z > 0$. We shall assume that the characteristic size k^{-1} of an inhomogeneity $\Delta\mathcal{H}$ satisfies the condition $z_1 \gg k^{-1} \gg z_2$. Then, the open and circular orbits make very different contributions to $f(\mathcal{H}+H_0)$.

The contribution of the circular orbits can be found by calculating the change in their revolution period T in a strongly inhomogeneous field. We shall represent T in the form

$$T = 4\frac{\partial}{\partial E}\int_{z_0}^{z_1} dz\,(E - U(z))^{1/2}, \qquad (8)$$

where $U(z) = [E^{1/2} - A(z)]^2$; $\frac{1}{2}mE$ is the electron energy; $mcA(z)/e$ is the vector potential of the magnetic field; $z_{0,1}$ are the roots of the equation $E = U(z)$. Then,

$$\Delta T = -2\frac{\partial}{\partial E}\int_{z_0}^{z_1} \frac{\Delta U\,dz}{(E - U_0(z))^{1/2}} \qquad (9)$$

[the perturbation $\Delta\mathcal{H}$ does not occur in $U_0(z)$].

When the time dependence is $\Delta\mathcal{H} \propto \Delta\mathcal{H}(0)e^{-ht}$, we find

from Eq. (7) that

$$\frac{\Delta T}{T} \sim -\frac{\Delta \mathcal{H}(0)}{\mathcal{H}} \cdot \frac{2}{3} \exp(-kz_1)[I_0(kz_1) - I_1(kz_1)], \quad (10)$$

where $I_n(x)$ is a Bessel function of the imaginary argument. In the limiting case of $kz_1 \gg 1$, we find from Eq. (10) that

$$\frac{\Delta T}{T} \sim -\frac{\Delta \mathcal{H}(0)}{\mathcal{H}} (kz_1)^{-3/2} \quad (11)$$

The corresponding contribution to $f(H)$ can, therefore, be $-\Delta\mathcal{H}(0)a(kz_1)^{-3/2}$, where a is a positive constant of the order of $(z_2/z_1)^{1/2}$. Using this expression in the equation $\mathcal{H} = f(H_0 + \mathcal{H})$, we obtain

$$1 = f' - bkz_2 - a(kz_1)^{-3/2}. \quad (12)$$

Since the nature of the spatial inhomogeneity corresponds to the conditions for the anomalous skin effect, the time dependence is governed by the factor $\exp(i\tilde{\omega}t)$, where $\tilde{\omega}$ obeys

$$\tilde{\omega} = -c^2 r k^3 / 3\pi^2 \sigma, \quad (13)$$

whereas the value of k has to be found from Eq. (12). We have used here an approximate expression for the effective conductivity in a strong magnetic field although it is inapplicable in the case of a cylindrical Fermi surface.[5] Its use can be justified by, for example, the existence of an additional noncylindrical part of the Fermi surface.

We shall now introduce a new variable $kz_1 = \rho e^{i\varphi}$, where $0 < \varphi < \pi/2$, and also the quantity $\tilde{b} = bz_2/z_1 \ll 1$. Separating the real and imaginary parts in Eq. (12), we obtain

$$\tilde{b}\rho \sin\varphi - a\rho^{-3/2} \sin(3\varphi/2) = 0, \quad (14)$$

$$\tilde{b}\rho \cos\varphi + a\rho^{-3/2} \cos(3\varphi/2) = f' - 1. \quad (15)$$

It follows from Eq. (14) that undamped oscillations corresponding to $\varphi = \pi/3$ appear for $\rho = \rho_0 = [2a/3^{1/2}\tilde{b}]^{2/5}$. If $\rho < \rho_0$, the oscillations decay with time but if $\rho > \rho_0$, they grow with time. It follows from Eq. (15) that in the case of undamped oscillations we have

$$f' - 1 = \tilde{b}\rho_0/2, \quad (16)$$

which determines the characteristic amplitude of the rf field H_0^{ch} above which we can expect spontaneous oscillations.

The solution obtained satisfies the earlier assumptions:

$$kz_1 \sim (z_1/z_2)^{1/5} \gg 1, \quad (17)$$

$$kz_2 \sim (z_2/z_1)^{4/5} \ll 1. \quad (18)$$

The frequency of undamped oscillations is

$$\tilde{\omega} \sim c^2/3\pi^2 \sigma z_1^{1/5} z_2^{4/5}. \quad (19)$$

Substituting in the above formula the values of the bismuth parameters[6] and bearing in mind that under typical experimental conditions we have $z_1 \sim 10^{-1}$ cm and $z_2 \sim 5 \times 10^{-3}$ cm, we find that the oscillation frequency is $\tilde{\omega} \sim 10^4$ sec^{-1} [it should be noted that although $z_1 \gg z_2$ under experimental conditions, the ratio of these two quantities is such that the condition (17) is not satisfied].

It follows from the above analysis that if $f' > 1$, either an aperiodic growing perturbation may transform a sample to a stable state or growing oscillations of the magnetic moment may be observed. The existence of steady-state oscillations can be determined experimentally, especially as it is not easy to satisfy the condition (17).

EXPERIMENTAL OBSERVATION OF SPONTANEOUS OSCILLATIONS IN BISMUTH

Spontaneous oscillations were studied in bismuth disks 17.8 mm in diameter. A disk was placed inside an inductance coil which was used to generate the rf ($5 \times 10^5 < \omega/2\pi < 5 \times 10^6$ Hz) field and to detect the resultant oscillations of the magnetic moment. The disk was immersed in superfluid helium, whose temperature was 1.3–1.5°K, but the temperature of the sample differed considerably from that of the helium bath because of the Kapitza jump. The power evolved in a sample in a given experiment could reach 1 W and under these conditions the temperature of the sample could rise by 0.5°K. The coil emf was supplied to the input of an oscillograph (for the display of oscillations on the screen) and to an rf spectrum analyzer. The pass band of this analyzer was 0.4×10^3 Hz, which made it possible to determine the dependence of the spectral density of these oscillations on the frequency in the range up to 10^5 Hz.

The oscillations were exhibited by the majority of the samples with the $c_3 \| \mathbf{n}$ orientation, where $\mathbf{n}$ is the normal to the disk plane. The oscillation frequencies were within the range 1–10 kHz and they depended on the previous history, temperature of the helium bath, and orientation of the crystallographic axes of a sample relative to the rf and static fields. Application of a weak magnetic field suppressed the oscillations (Fig. 8) but at high amplitudes of the rf field the oscillations were observed not only in zero external field but also in the region corresponding to a side (located some distance from the origin) hysteresis loop.

The spontaneous oscillations were usually nonmonochromatic. An example is shown in Fig. 9. It can be seen from this figure that an increase in the rf field amplitude increased the oscillation frequency. This behavior was characteristic of all the samples. In

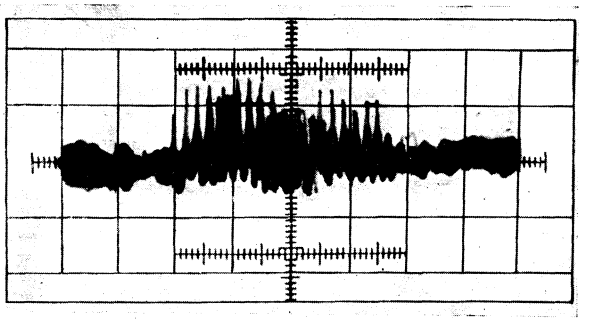

FIG. 8. Photograph taken from the oscillograph screen for a sample 0.54 mm thick investigated under the following conditions: $\omega/2\pi = 2 \times 10^6$ Hz, $H_0 = 1.15 \cdot \cos \Omega t$ Oe, $\Omega/2\pi = 40$ Hz, $H_\sim = 37.5$ Oe. The spontaneous oscillations can be seen and these are suppressed on increase of the magnetic field.

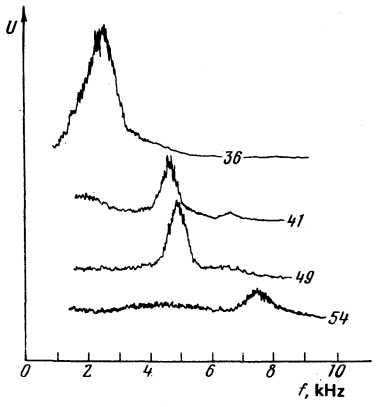

FIG. 9. Spectrum of the spontaneous oscillations in a sample 1 mm thick for $\mathbf{j} \| c_1$ and $\omega/2\pi = 1.6 \times 10^6$Hz. The rf field amplitude in oersted is given alongside each curve.

some cases the oscillations appeared in two ranges of $H_\sim$ and in each of them the frequency rose on increase of the rf field amplitude. Clearly, this increase in the frequency was associated with the field $\mathcal{H}$ and with a reduction in the characteristic dimensions z_1 and z_2.

Our measurements were carried out on three samples of identical quality and with the same orientations of the crystallographic axes. These samples differed in respect of the thickness, which was 0.54, 1.0, and 1.0 mm. The rf current was directed along the c_1 axis and the static magnetic field was perpendicular to the current. Under these conditions the critical values of the rf field $H_\sim^{cr}$ were 17.6, 13.2, and 6.5 Oe. The characteristic field $H_\sim^h$ in which a hysteresis loop appeared in zero magnetic field was the same for all samples: ~4 Oe. According to Eq. (16), at the moment of appearance of the spontaneous oscillations the condition $f' - 1 \ll 1$ should be satisfied, i.e., the field should differ negligibly from $H_\sim^h$ ($H_\sim^h$ corresponds to $f' = 1$).

As pointed out above, an important requirement for the appearance of the oscillations is that an electron following the usual circular orbit can return to the skin layer. In other words, the orbit diameter should be less than the thickness of the sample. It is possible that the increase of $H_\sim^{cr}$ for the thinner samples is due to the cutoff of the electron orbits in weak fields $H_\sim$. When the amplitude of the hf field becomes such that $\mathcal{H}(H_\sim)$ satisfies the condition $\mathcal{H} = 2v_F mc/ed$, spontaneous oscillations should be observed.

The oscillation amplitude was estimated from the emf that appeared in the detection coil. Conversion of the value of δ from Ref. 7 in accordance with the anomalous skin effect formulas gave the value of 10^{-2}cm at 10^3 Hz. Use of this value gave $\Delta\mathcal{H}(0)$, which was 1 Oe for $H_\sim \sim 20$ Oe.

CONCLUSIONS

Our experimental calculations demonstrate that the rectification in a metal subjected to rf and weak static magnetic fields is due to the influence of the rf magnetic field on the electron trajectories. Depending on the external magnetic field, the usual Larmor orbit may be slightly distorted or a new orbit may appear. Allowance for this influence makes it possible to predict qualitatively the dependence of the magnetic moment of a sample on the external magnetic field and to understand the reasons for the appearance of the current states. A more rigorous calculation allowing for the mutual influence of the various electron groups yields not only the dependence of the width of a hysteresis loop in bismuth on the direction of the magnetic field, which is in qualitative agreement with the experimental results, but also makes it possible to explain a finer effect, which is the appearance of a side hysteresis loop. An analysis of this type of nonlinearity makes it also possible to predict the appearance of spontaneous oscillations of the magnetic moment detected experimentally.

The authors are deeply grateful to V. F. Gantmakher for valuable discussions, to L. B. Davydova for her help in the numerical calculations, and to L. P. Mezhov-Deglin for technical help.

[1]V. T Dolgopolov, Zh Eksp. Teor. Fiz. **68**, 355 (1975) [Sov. Phys. JETP **41**, 173 (1975)].
[2]V. T. Dolgopolov and S. S. Murzin, Pis'ma Zh. Eksp. Teor. Fiz. **23**, 213 (1976) [JETP Lett. **23**, 190 (1976)].
[3]G. I Babkin and V. T. Dolgopolov, Solid State Commun. **18**, 713 (1976).
[4]L. É. Gurevich and I. V. Ioffe, Zh. Eksp. Teor. Fiz. **62**, 1531 (1972); **61**, 1133 (1971); **58**, 2047 (1970); **59**, 1409 (1970) [Sov. Phys. JETP **35**, 803 (1972); **34**, 605 (1972); **31**, 1102 (1970); **32**, 769 (1971)].
[5]É. A. Kaner and V. F. Gantmakher, Usp. Fiz. Nauk **94**, 193 (1968) [Sov. Phys. Usp. **11**, 81 (1968)].
[6]V. S. Édel'man, Usp. Fiz. Nauk 123, 257 (1977) [Sov. Phys. Usp. **20**, 819 (1977)].
[7]G. E. Smith, Phys. Rev. **115**, 1561 (1959).

Translated by A. Tybulewicz